

EFFECT OF BINARY BASICITY ON CHROMIUM OCCURRENCE IN STAINLESS STEEL SLAG

Q. Zeng ^a, J.-L. Li ^{a, b, c,*}, G.-J. Ma ^a, H.-Y. Zhu ^a

^a The State Key Laboratory of Refractories and Metallurgy, Wuhan University of Science and Technology, Wuhan, China

^b Hubei Provincial Key Laboratory for New Processes of Ironmaking and Steelmaking, Wuhan University of Science and Technology, Wuhan, China

^c Key Laboratory for Ferrous Metallurgy and Resources Utilization of Ministry of Education, Wuhan University of Science and Technology, Wuhan, China

(Received 04 March 2021; Accepted 05 August 2021)

Abstract

Comprehensive utilization of stainless-steel slag (SSS) is restrained due to the risk of Cr⁶⁺ leaching. Based on the studying the microstructure of synthetic slag (SS) containing Cr₂O₃ with XRD, SEM-EDS, and Image pro, the effect of binary basicity on the chromium occurrence in SSS was investigated. The results indicated that the binary basicity had a significant impact on the properties of spinel crystals. There was a positive correlation between the calcium content in spinel crystals and the SS basicity. The size of spinel crystals varied from large to small and the precipitation occurrence changed with the basicity increase. Furthermore, the chromium occurrences changed with the basicity. The chromium was produced in spinel crystals at lower basicity, but as the basicity increased to 3.0, the chromium precipitated as calcium chromate. In view of the relationship between the chromium leaching behavior and its occurrence, increasing basicity raised the Cr⁶⁺ leaching.

Keywords: Stainless steel slag (SSS); Hexavalent chromium; Spinel crystals; Binary basicity

1. Introduction

The stainless steel production was 50.892 million metric tons in 2020, and the Chinese production was 30.139 million metric tons. SSS as by-product in the stainless steel production, its output is about 25 wt% of the total stainless steel amount, which means the Chinese SSS production was about 7.53 million tons [1, 2]. At present, Chinese stainless-steel plants merely recover valuable metals such as iron, chromium, and nickel through a grinding process, and parts of tailing slags can be applied as subgrade material, concrete aggregate, cement production, brick and block making, sintering for iron making and other materials. The rest tailing slags are stored as stacking or landfill. These materials and tailing slags containing chromium are able to leach Cr⁶⁺. Cr⁶⁺ which were reported to pollute the environment and cause human poisoning and carcinogenesis [3-8]. Therefore, to achieve the comprehensive utilization of SSS and enhance economic benefits, it is necessary to solve the Cr⁶⁺ leaching issue and ensure the safety of SSS products for long-term applications.

The limitation of Cr⁶⁺ leaching from SSS is a

significant challenge. Previous research implied three main measures to control the Cr⁶⁺ leaching: the addition of reductive compounds in the application of SSS, the adjustment of cooling regimes, and the modified components to transform the Cr occurrence. The reductive compounds, such as FeSO₄, can limit the Cr⁶⁺ leaching by chemical reduction of the oxidized Cr⁶⁺ to the nontoxic Cr³⁺ or Cr [9]. Nevertheless, this Cr⁶⁺ inhibition method is time-dependent and cannot ensure the long-term safety of SSS products. The rapid cooling approach includes two beneficial aspects: first, it promotes the formation of the glass phase and fixes heavy metal elements, such as Cr [10]; second, Cr⁶⁺ is stable only at temperatures lower than 1228 °C because of the different precipitated phases, so the rapid cooling rate restrains the amount of Cr⁶⁺ [11, 12]. The final measure is the transformation of the Cr occurrence, which is divided into an enriched state and dispersed state, to limit the Cr⁶⁺ leaching. The enriched state refers to Cr existing in spinel crystals, and the dispersed state includes an isomorphous solid solution and micro-inclusion. The structure of spinel crystals is Me^IOMe^{II}₂O₃, in which Me^I is a divalent

*Corresponding author: jli@wust.edu.cn



metal ion, including Mg^{2+} , Fe^{2+} , Mn^{2+} , and Me^{II} is a trivalent metal ion, including Cr^{3+} , Al^{3+} , and Fe^{3+} [13]. Spinel crystals limit the leachability but also enhance the Cr oxidation resistance, and they are considered as a suitable mineral phase for Cr fixing. As such dispersed Cr is unstable, the Cr^{6+} leaching is negatively affected by the dissolution of matrix minerals [14-17].

Cao and Zhao [18, 19] analyzed the stability of 1.0, 1.5, 2.0 slags basicity with 5% Cr_2O_3 content, and found that the spinel phase was not obviously damaged in SEM pictures, and the periclase phase disappeared after the leaching tests in the leaching solution of pH = 3.2. And the silicate phase was not able to limit the leaching of Cr^{6+} . The leaching amount of Cr^{6+} was very low at 1600 °C, which was 2.82 mg/L, 2.26 mg/L, and 3.68 mg/L, respectively, due to the existence of spinel phase. Spinel crystals further grew, and the leaching amount of Cr^{6+} decreased to 1.78 mg/L, 0.62 mg/L, and 1.46 mg/L, respectively, as the temperature decreased to 1300 °C. Cao [20] studies on growth behavior of spinel in SSS during cooling process further indicated that the leaching amount of chromium could be reduced to less than 0.01 mg/L by controlling the cooling condition to promote the growth of spinel crystals. Esfahani [21] investigated the effect of composition on the crystallization behavior and found the crystalline phases were translucent and the nucleation was limited to grow larger crystals at low basicity. Albertsson [22] found the range 1.0-1.4 of basicity of CaO-MgO-SiO₂-Cr₂O₃ synthetic slag was favoured to control the precipitation of Cr-spinel. The precipitation of spinel crystals is also affected by the oxygen partial pressure. Albertsson [23] did the low oxygen partial pressure on the chromium partition in CaO-MgO-SiO₂-Cr₂O₃-Al₂O₃ at elevated temperatures. It was found that low oxygen partial pressure had a strong impact on chromium partition.

In our previous study, the leaching experiments were performed on SSS with different basicity (the ratio of CaO% and SiO₂% was 1.25~1.89). It was confirmed that the Cr^{6+} leaching was higher for the sample with low Cr_2O_3 content and high basicity than for the sample with high Cr_2O_3 content and low basicity, which implied a good agreement between the Cr stability and the occurrence state [24]. CaO-Al₂O₃-MgO-SiO₂-Cr₂O₃ slag with varied CaO/SiO₂ (1.1, 1.3, 1.5) was studied at 1673K by Shu [25], the results showed the biggest size of spinel crystal at 1.5 basicity and Cr is enriched in spinel phase and liquid phase. Liu found that the presence of solid particles in slag has a critical influence on the viscosity at high basicity [26]. However, the effect of basicity and Cr_2O_3 content on viscosity was nonlinear at low or high basicity. Hence, the viscosity change caused by the effect of compositions and basicity has no

objective law. For the actual complex SSS composed of multi-component oxides, specific problems need to be analyzed in detail. The general idea is to promote the formation of spinel phase, the enrichment of Cr in spinel phase, and then reduce the leaching amount of Cr. In this paper, the effect of binary basicity (CaO%/SiO₂%) on the chromium occurrence in SSS by thermodynamic calculations and theoretical analysis of synthetic slag (SS) was investigated. The element distribution in spinel phase was further analyzed and its formation mechanism was explained.

2. Experimental

CaO, SiO₂, MgO, Al₂O₃, Cr₂O₃, FeC₂O₄·2H₂O, and H₃BO₃ were used as raw materials for SS. All reagents were of analytical grade (AR) produced by Sinopharm group. The specific focuses were that FeO was replaced by FeC₂O₄·2H₂O and 0.1 wt % H₃BO₃ was added into the SS to form a block sample.

Based on the chemical composition of EAF smelting SSS, the CaO-SiO₂-MgO-Al₂O₃-Cr₂O₃-FeO slag system was designed, and the basicity (CaO%/SiO₂%) was from 0.6 to 3.0. According to the chemical composition shown in Table 1, the reagent powder was accurately weighed by electronic balance, sieved (Φ 0.55mm) for 4 - 6 times, and then ground by grinder (YP200) to mix fully. The mixture was put into molybdenum crucible (Φ 60 x 110) and melted in a high-temperature carbon tube furnace (25 kW, 1650 °C). The heating regime was heating to 1550 °C at the rate of 10 °C/min in the nitrogen (3L/min) atmosphere, and held for 30 min. The sample was quenched in water.

A scanning electron microscope (NanoSEM400) was used to investigate the microstructure and the morphology, and EDS analysis was used to determine the chemical composition by line scanning and the mapping of the elements. XRD (X-Pert Pro MPD) was used to analyze the mineral phase after grinding. The particle size of the spinel crystal in the sample was calculated based on the SEM micrographs using Image-Pro Plus (IPP 6.0) image analysis software, and 10 fields of the same magnification were randomly selected for each sample to obtain a statistically relevant analysis. The Reaction module of FactSage 7.3 was used to calculate the thermochemical properties.

Table 1. Chemical composition of SS/wt %.

No.	CaO	SiO ₂	MgO	Al ₂ O ₃	Cr ₂ O ₃	FeO	CaO%/SiO ₂ %
SS1	29.25	48.75	8.00	8.00	6.00	8.00	0.60
SS2	45.50	32.50	8.00	8.00	6.00	8.00	1.40
SS3	50.14	27.86	8.00	8.00	6.00	8.00	1.80
SS4	53.63	24.38	8.00	8.00	6.00	8.00	2.20
SS5	58.50	19.50	8.00	8.00	6.00	8.00	3.00



3. Results and Discussion

3.1. Effect of basicity on the microstructure and morphology of SS

Combined SEM micrographs (Fig.1) and XRD patterns (Fig.2) imply that the mineral phases of SS containing Cr_2O_3 transform obviously with the increase of basicity. The microstructure of SS1 is composed of spinel crystals, $\text{Ca}(\text{Mg,Fe})\text{Si}_2\text{O}_4$, and silicate matrix, then, the microstructure of SS3 is similar to that of SS1, but $\text{Ca}(\text{Mg,Fe})\text{Si}_2\text{O}_4$ is completely transformed to $\text{Ca}_2\text{MgSi}_2\text{O}_7$. The microstructure of SS4 is composed of $\text{Ca}_3\text{MgSi}_2\text{O}_8$ and $(\text{Mg}_x\text{Fe}_{1-x})\text{O}$ spinel crystals. Ca_2SiO_4 , $(\text{Mg}_x\text{Fe}_{1-x})\text{O}$, and CaCr_2O_4 are mineral phases present in the SS5 sample with the highest 3.0 basicity. Wu found that as the FeO content of the slag system was invariant, and in the basicity range of 1.0-1.5 ($\text{CaO}\% / \text{SiO}_2\%$), spinel solid solutions of (Mg, Fe) ($\text{Fe, Al, Cr})_2\text{O}_4$ were formed in each sample [27]. In that study, the size of the spinel crystal with a regular shape is negatively related to basicity, spinel crystal could be produced only when the basicity is lower than 1.8. The average size of spinel crystals in SS1 was $12.30\ \mu\text{m}$, and it reduces to $4.47\ \mu\text{m}$ in SS3. On the contrary, Cr does not precipitate anymore in the spinel crystals, but in the form of CaCr_2O_4 in SS5. Li studied the Cr distribution and enrichment in the $\text{CaO-Al}_2\text{O}_3\text{-MgO-}$

$\text{SiO}_2\text{-CrO}_x\text{-Fe}_x\text{O}$ slag system with $0.96\sim 1.96$ basicity [28], and their results showed that the Cr was enriched in CaCr_2O_4 at high basicity, and in spinel crystals at low basicity. Compared with Fig.1 and Fig.2, the main silicate phases in SS are $\text{Ca}(\text{Mg,Fe})\text{Si}_2\text{O}_4$, $\text{Ca}_2\text{MgSi}_2\text{O}_7$, $\text{Ca}_3\text{MgSi}_2\text{O}_8$, and Ca_2SiO_4 .

The investigation of the effect of FeO on the stability of spinel crystal showed that the spinel crystal was an octahedral $\text{Mg}_{1-x}\text{Fe}_x\text{Fe}_2\text{O}_4$ solid solution [29], with the shape of the spinel crystal similar to that shown in Fig.1. The spinel crystal

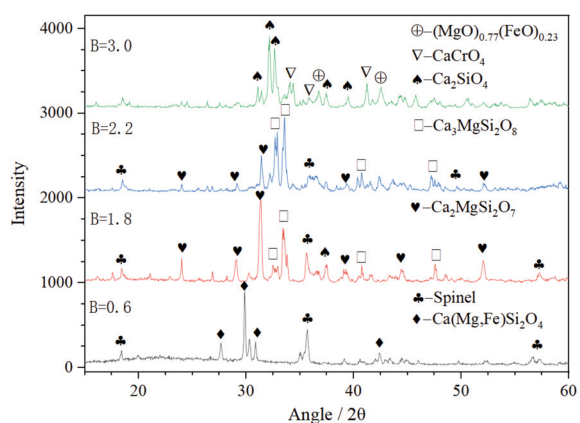


Figure 2. XRD patterns of SS

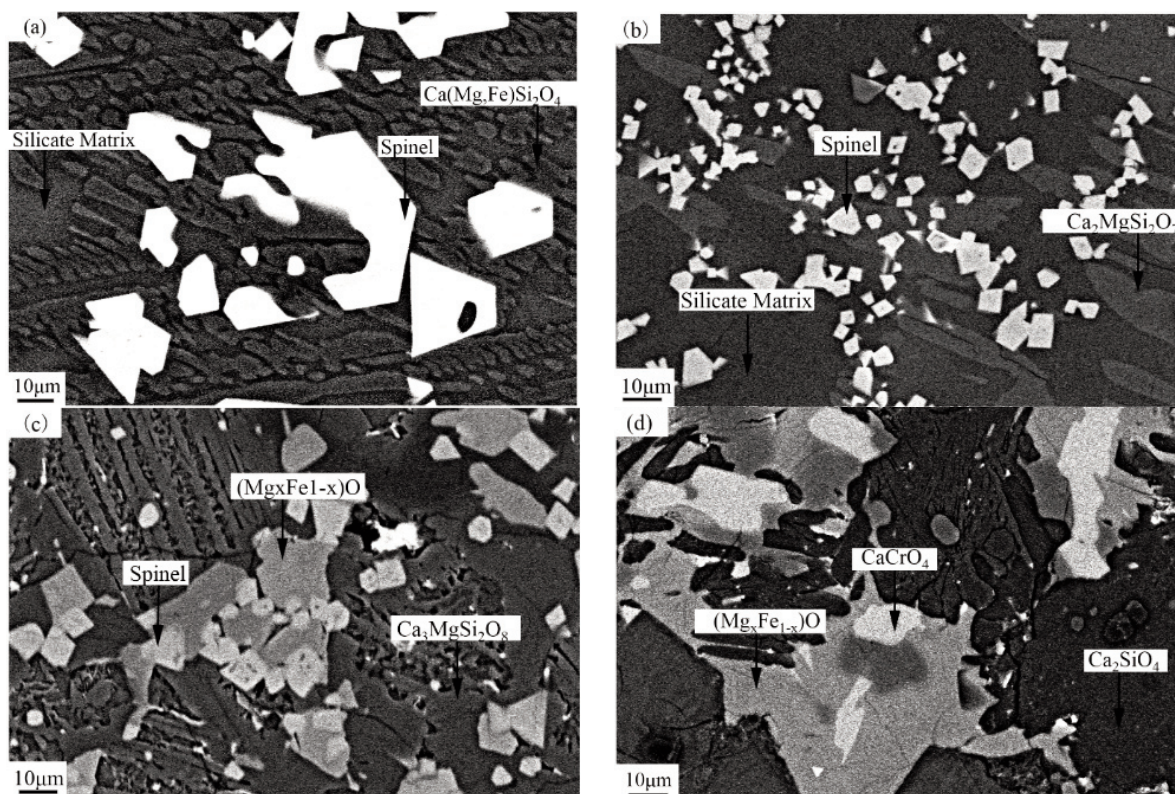


Figure 1. Microstructures of SS with different basicity: (a), (b), (c), and (d) represent the slag samples with the basicity 0.6, 1.8, 2.2, and 3.0, respectively

embedded in the matrix or silicate phase is represented by a light-colored feature in the SEM micrograph. After the sample preparation, the interface between the spinel crystal and the matrix, or silicate phase, should be a regular straight line. As shown in Fig.1 (a), the hole-like feature that looks like the giant spinel crystal is $\text{Ca}(\text{Mg,Fe})\text{Si}_2\text{O}_4$, and the matrix or silicate phase in the complete section at the lower right corner. That means the spinel crystals have been completely crystallized. Similar features occur for the spinel crystals in the central region of Fig.1 (c). The Cr^{6+} leaching mechanism proposed by Pillay assumes the reaction at the contact interface of CaO and Cr_2O_3 to yield CaCrO_4 [9]. Although kinetics conditions of molten SSS at low basicity is better, the growth of a spinel crystal that belongs to a substitutional solid solution is restricted by the activity of substituting elements. However, the leaching risk might increase in the case of incompletely grown spinel crystals. As we have seen above, the number of mineral phases increases with the basicity. The spinel crystals exhibit the central defect, Fig.1(c), and at the basicity of 3.0, there is no spinel phase in SS5. In summary, the low basicity of 1.8 is suitable for the formation of spinel crystals

3.2. Effect of basicity on the chromium occurrence

Concerning to the EDS results, the Cr occurrence has been assessed. The elemental mapping of Cr and Ca is shown in Fig.3, with the basicity of 0.6, 1.4, and 3.0. The chemical compositions of different mineral

phases are summarized in Table 2. The SS1 microstructure can be divided into three distinct phases. Among them, the white area with a regular shape is the spinel crystal, and the elemental mapping supports this observation. Cr mainly enriches the spinel crystal, while Ca exists only in the non-spinel mineral phase. The content of the elements differs significantly between the areas, having a well-defined boundary. This is also consistent with the line scanning observation in Fig. 4, which shows the step mutation curves of Cr and Ca contents in different precipitates.

At the basicity of 0.6, the spinel crystal is enriched in Cr, while Ca is contained in the non-spinel mineral phase in SS2. Compared with SS1, the characteristics of the element occurrence in SS2 are reflected at the boundary of spinel crystals. Fig. 4 shows that there is a tiny compositional decreasing gradient of Ca distribution towards the interior of spinel crystals near the spinel crystal surface, within which the element weights of Ca and Cr are in negative correlation. As shown in Table 2, the Ca content of spinel crystals in SS1 and SS2 are 0.40 at% and 0.85 at%, respectively, while the Cr content is 27.11 at% and 19.98 at%.

In comparison with the other samples, the distribution of Cr and Ca changes considerably in SS5 at the basicity of 3.0. Fig.5 shows that Ca exists along the entire scanning line, while Cr is mainly concentrated in the bright white and gray-white areas. The Cr content in the gray area is 2.70 at%, and the black area has the lowest Cr content of only 0.05 at%. The SS5 differs from the lower basicity samples by the coexistence of Ca and Cr, with CaCr_2O_4 and

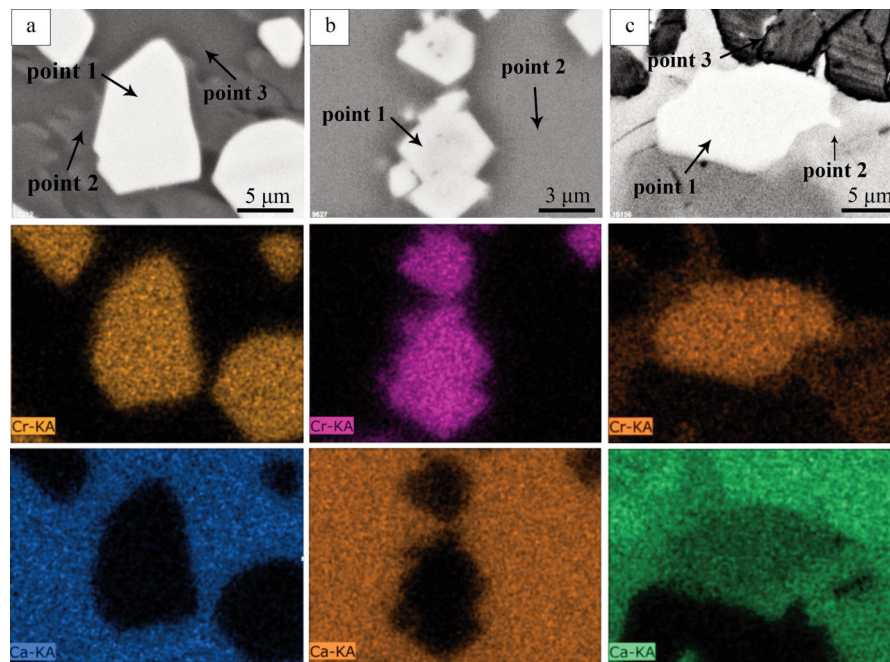
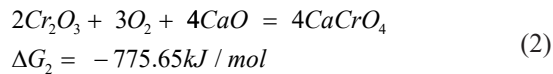
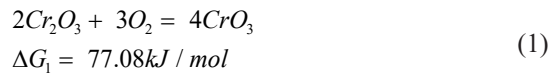


Figure 3. The elemental mapping of the spinel crystal with different basicity: (a), (b), and (c) represent the slag samples with the basicity 0.6, 1.4, and 3.0, respectively

Ca_2SiO_4 , which reduces the Cr stability in SS and increases the risk of Cr leaching.

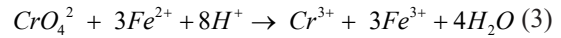
3.3. Effect of microstructure on the Cr^{6+} leaching

The natural Cr^{6+} leaching is determined by the microstructure of the mineral phase of SSS. The standard Gibbs free energy (ΔG) of Cr^{6+} in standard conditions, 25°C and 100kPa, is calculated by FactSage 7.3 as follows:



As we can see in Eq.1, the reaction of Cr_2O_3 and O_2 is not spontaneous, but it becomes spontaneous when CaO is present, as Eq.2. Compared with the elemental scanning lines in Fig. 4 and Fig. 5, Cr in the matrix or CaCrO_4 phase is in direct contact with CaO or calcium silicate around it, which increases the feasibility of the reaction. The solubility of CaCrO_4 in water at 20 °C is 2.25g. The natural SSS leaching model is an irreversible unreacted core model, and Eq. 2 determines the leaching rate. There is almost no Ca element in the spinel crystal, and Cr in the spinel phase is trivalent. The oxidation of trivalent Cr^{3+} to hexavalent Cr^{6+} requires an increased oxygen partial pressure, the activity of Cr_2O_3 , and lattice damage of spinel. Therefore, Cr in spinel does not oxidize readily. Cr^{6+} in acidic solutions is related to its concentration and the pH value [30]. Under acidic

conditions, Cr^{6+} can be reduced to Cr^{3+} in the presence of Fe^{2+} , as Eq. 3 [31], which indicates that the spinel crystal has good resistance to natural leaching of Cr^{6+} , although the crystal structure is damaged.



The transform between bivalent and trivalent of Cr is as Equation (4),(5).



The transform between trivalent and hexavalent of Cr is as Equation(6),(7).



Nell and De Villiers studied the distribution of chromium in $\text{CaO-CrO-Cr}_2\text{O}_3\text{-SiO}_2$ under low oxygen partial pressure, and found that the Cr were main in the $\text{CaCr}^{2+}\text{Si}_4\text{O}_{10}$ and $(\text{Ca}_{0.4}\text{Cr}_{0.6}^{2+})\text{Cr}_2^{3+}\text{O}_4$. These phases can react to produce more oxidation phases, and improve the temperature of liquid line at lower oxygen partial pressure [32]. Mirzayouf studied the CaO-SiO-CrOx and found that the value of $\text{Cr}^{3+}/\text{Cr}^{2+}$ in the system increased with the increase of oxygen partial pressure at 1600°C and low oxygen partial pressure, and the increase of basicity also led to the decrease of Cr content. Cr^{6+} content will increase with the increase of oxygen partial pressure, and the

Table 2. Chemical composition of each precipitate in Fig.3 /at%

basicity	precipitation	O	Cr	Ca	Fe	Mg	Si
B=0.6	White (P.1)	56.66	27.11	0.4	8.41	6.91	0.06
	Gray (P.2)	59.28	0.97	35674	1.51	8.58	18.12
	Matrix (P.3)	59.66	0.21	10.43	1.12	1.00	22.33
B=1.4	White (P.1)	60.93	19.98	0.85	4.78	9.00	0.02
	Matrix (P.2)	57.86	0.08	19.28	2.20	3.89	12.94
B=3.0	White (P.1)	58.39	20.21	16.71	2.82	1.63	0.08
	Gray (P.2)	54.89	2.70	8.57	14.03	18.78	0.07
	Black (P.3)	57.28	0.05	30.36	0.18	0.09	11.72

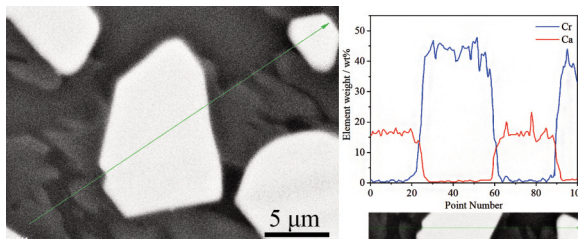


Figure 4. Chemical composition change behavior in local area of SS1

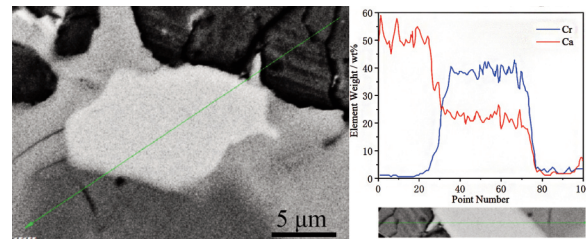


Figure 5. Chemical composition change behavior of spinel crystal interface in SS4

increase of basicity will increase the content of Cr^{6+} under the condition of high oxygen partial pressure [33].

Cr occurrence is the decisive factor for the Cr^{6+} leaching. The typical mineral phases in the EAF SSS include merwinite ($\text{Ca}_3\text{MgSi}_2\text{O}_8$), anorthite ($\text{Ca}_2\text{MgSi}_2\text{O}_7$), gehlenite ($\text{Ca}_2\text{Al}_2\text{SiO}_7$), dicalcium silicate (Ca_2SiO_4), spinel crystals, and simple oxide solid solution (MeO) [18, 34]. Spinel crystals and MeO phases are considered to be available mineral phases for Cr solidification, which cannot only inhibit the oxidation of Cr_2O_3 , but they are also poorly soluble in water. Minerals such as dicalcium silicate, merwinite, and melilitite easily dissolve in water, so Cr leaches with the dissolution of these minerals. Garcia-Ramos stabilized Cr_2O_3 by adding Al_2O_3 or MgO to the CaO-SiO₂-Cr₂O₃ slag system [16]. The results showed that calcium chromite (CaCr_2O_4) was produced with no Al_2O_3 or MgO added. After the Al_2O_3 or MgO addition, the CaCr_2O_4 phase disappeared, and the Cr leaching was significantly decreased. It must also be mentioned that the Cr solubility in industrial slag is mainly affected by basicity and MgO content. Given that Cr in calcium dichromate (CaCr_2O_4) easily dissolves in acid rain, as the basicity is about 2.2, and CaCr_2O_4 oxidizes to calcium chromate (CaCrO_4) in the slag yard. The Cr solubility is further enhanced because CaCrO_4 is more soluble in the aqueous solution. Hence, the rise of basicity is increasing the Cr leaching risk in SSS.

4. Conclusions

The effect of binary basicity on Cr occurrence in SSS was investigated using. The main conclusions can be represented as follows:

(1) The size of spinel crystals varied from large to small, and the precipitated phases changed with the increase of SS basicity. The main silicate species evolved from $\text{Ca}(\text{Mg,Fe})\text{Si}_2\text{O}_4$, $\text{Ca}_2\text{MgSi}_2\text{O}_7$, $\text{Ca}_3\text{MgSi}_2\text{O}_8$, and Ca_2SiO_4 .

(2) Basicity changed the Ca content in the spinel crystal and at the interface between spinel crystal and silicate phase. Thus, the phase interface between the spinel crystal and the silicate phase is gradually blurred.

(3) Basicity changed the Cr occurrence as well. Cr was mainly in the spinel crystals at lower basicity. Still, the Cr content in the precipitated phases increased with the basicity. Once the basicity was 3.0, Cr precipitated in the form of CaCrO_4 . The higher basicity such as 3.0 enhances the risk of leaching without spinel crystals in slag. Due to the incomplete spinel crystals at lower basicity, it is a feasible range of basicity from 1.8 to 2.2 to product spinel crystals to control the leaching of Cr^{6+} .

Acknowledgements

This work was financially supported by the National Natural Science Foundation of China (No. 51974210), Hubei Provincial Natural Science Foundation (No.2019CFB697), and State Key Laboratory of Refractories and Metallurgy, Wuhan University of Science and Technology.

Author Contributions

Conceptualization: J.-L. Li. and Q. Zeng.; Methodology: G. Ma.; Software: Q. Zeng.; Writing—review and editing: Q. Zeng.; Project administration: H.-Y. Zhu.; Funding acquisition: J.-L. Li. All authors have read and agreed to the published version of the manuscript.

Conflict of Interest

The authors declare that they have no conflict of interest.

References

- [1] ISSF(2020). Stainless steel production decreases by 2.5% to 50.9 million tons in 2020. <https://www.worldstainless.org/news/stainless-steel-production-decreases-by-2-5-to-50-9-million-tons-in-2020/>
- [2] W. Han, The hydro-processing of stainless steel slag and its application in baosteel, Baosteel Technology (in China), 3 (2010) 30-33. <https://doi.org/CNKI:SUN:BGJS.0.2010-03-008>
- [3] L. M. Sánchez, Á. M. Ubios, Alterations in odonto genesis and tooth eruption resulting from exposure to hexavalent chromium in suckling animals, International Journal of Paediatric Dentistry, 30 (1) (2020) 35-41. <https://doi.org/10.1111/ipd.12573>
- [4] W. Li, X. Xue, Effect of cooling regime on phase transformation and chromium enrichment in stainless-steel slag, Ironmaking & Steelmaking, 46 (7) (2018) 1-7. <https://doi.org/10.1080/03019233.2018.1436890>
- [5] S. S. Biswal, P. Chittaranjan, S. Sudarsan, Entrapment of chromium in cement with waste material, Materials Today: Proceedings. 35 (2) (2020) 112-117. <https://doi.org/10.1016/j.matpr.2020.03.326>
- [6] F. Saly, L. Guo, R. Ma, Properties of steel slag and stainless steel slag as cement replacement materials: a comparative study, Journal of Wuhan University of Technology, 33 (2018) 1444-1451. <https://doi.org/10.1007/s11595-018-1989-3>
- [7] Y. Chen, D. An, S. Sun, Reduction and removal of chromium VI in water by powdered activated carbon, Materials (Basel), 11 (2) (2018) 269. <https://doi.org/10.3390/ma11020269>
- [8] J. Rosales, F. Agrela, J. A. Entrenas, Potential of stainless steel slag waste in manufacturing self-compacting concrete, Materials, 13 (9) (2020) 2049. <https://doi.org/10.3390/ma13092049>
- [9] K. Pillay, H. Blottnitz, J. Petersen, Ageing of chromium(III)-bearing slag and its relation to the



- atmospheric oxidation of solid chromium(III)-oxide in the presence of calcium oxide, *Chemosphere*, 52 (10) (2003) 1771-1779.
[https://doi.org/10.1016/S0045-6535\(03\)00453-3](https://doi.org/10.1016/S0045-6535(03)00453-3)
- [10] M. Baghalha, V. G. Papangelakis, W. Curlook, Factors affecting the leachability of Ni/Co/Cu slags at high temperature, *Hydrometallurgy*, 85 (1) (2007) 42-52.
<https://doi.org/10.1016/j.hydromet.2006.07.007>
- [11] Y. Lee, C. L. Nassaralla, Formation of hexavalent chromium by reaction between slag and magnesite-chrome refractory, *Metallurgical & Materials Transactions B*, 29 (2) (1998) 405-410.
<https://doi.org/10.1007/s11663-998-0117-8>
- [12] Y. Lee, C. L. Nassaralla, Minimization of hexavalent chromium in magnesite-chrome refractory, *Metallurgical & Materials Transactions B*, 28 (5) (1997) 855-859. <https://doi.org/10.1007/s11663-997-0013-7>
- [13] P. Drissen, A. Ehrenberg, M. Kühn, Recent development in slag treatment and dust recycling, *Steel Research International*, 80 (10) (2010) 737-745.
<https://doi.org/10.2374/SRI09SP055>
- [14] R. B. Dean, Hazardous industrial waste management and testing: third symposium, 3 (4) (1985) 399
[https://doi.org/10.1016/0734-242X\(85\)90133-8](https://doi.org/10.1016/0734-242X(85)90133-8).
- [15] H. Cabrera-Real, A. Romero-Serrano, Effect of MgO and CaO/SiO₂ on the immobilization of chromium in synthetic slags, *Journal of Material Cycles & Waste Management* 14 (4) (2012) 317-324.
<https://doi.org/10.1007/s10163-012-0072-y>
- [16] E. García. Ramos, A. Romero. Serrano, B. Zeifert, Immobilization of chromium in slags using MgO and Al₂O₃, *Steel Research International*, 79 (5) (2008) 332-339. <https://doi.org/10.1002/srin.200806135>
- [17] S. Yusuke, M. Takahiro, H. Mitsutaka, Prevention of chromium elution from stainless steel slag into seawater, *ISIJ International*, 51 (5) (2011) 728-732.
<https://doi.org/10.2355/isijinternational.51.728>
- [18] L. H. Cao, C. J. Liu, Q. Zhao, Analysis on the stability of chromium in mineral phases in stainless steel slag, *Metallurgical Research & Technology*, 115 (1) (2017) 114. <https://doi.org/10.1051/metal/2017071>
- [19] Q. Zhao, C. Liu, L. H. Cao, Effect of lime on stability of chromium in stainless steel slag, *Minerals*, 8 (2018) 424-434. <https://doi.org/10.3390/min8100424>
- [20] L. H. Cao, C. J. Liu, Q. Zhao, Growth behavior of spinel in stainless steel slag during cooling process, *Journal of Iron and Steel Research International*, 25 (11) (2018) 1-9. <https://doi.org/10.1007/s42243-018-0058-7>
- [21] S. Esfahani, M. Barati, Effect of slag composition on the crystallization of synthetic CaO-SiO₂-Al₂O₃-MgO slags: part I—crystallization behavior, *Journal of Non-Crystalline Solids*, 436 (2016) 35-43.
<https://doi.org/10.1016/j.jnoncrysol.2015.12.011>
- [22] G. Albertsson, L. Teng, B. Bjorkman, Effect of basicity on chromium partition in CaO-MgO-SiO₂-Cr₂O₃ synthetic slag at 1873 K, *Mineral Processing and Extractive Metallurgy*, 123 (2) (2014) 116-122.
<https://doi.org/10.1179/1743285513Y.0000000038>
- [23] G. Albertsson, L. Teng, B. Bjorkman, S. Seetharaman, F. Engstrom, Effect of low oxygen partial pressure on the chromium partition in CaO-MgO-SiO₂-Cr₂O₃-Al₂O₃ synthetic slag at elevated temperatures, *Steel Research International*, 84 (7) (2013) 670-679.
<https://doi.org/10.1002/srin.201200214>
- [24] Y. Lin, Q. Luo, B. Yan, Effect of B₂O₃ addition on mineralogical phases and leaching behavior of synthetic CaO-SiO₂-MgO-Al₂O₃-CrOx slag, *Journal of Material Cycles and Waste Management*, 22 (4) (2020). <https://doi.org/10.1007/s10163-020-01015-4>
- [25] Q. Shu, Q. Luo, L. Wang, Effects of MnO and CaO/SiO₂ mass ratio on phase formations of CaO-Al₂O₃-MgO-SiO₂-CrOx slag at 1673K and PO₂=10-10 atm, *Steel Research International*, 86 (4) (2015) 391-399. <https://doi.org/10.1002/srin.201400117>
- [26] Z. Liu, R. Dekkers, B. Blanpain, Experimental study on the viscosity of stainless steelmaking slags. *ISIJ International*, 59 (3) (2019) 404-411.
<https://doi.org/10.2355/isijinternational.ISIJINT-2018-558>
- [27] X. Wu, X. Dong, R. Wang, Crystallization behaviour of chromium in stainless steel slag: effect of FeO and basicity, *Journal of Residuals Science & Technology*, 13 (2016) S57-S62.
<https://doi.org/10.12783/issn.1544-8053/13/S1/10>
- [28] W. Li, X. Xue, Effects of silica addition on chromium distribution in stainless-steel slag, *Ironmaking & Steelmaking*, 45 (10) (2018) 929-936.
<https://doi.org/10.1080/03019233.2017.1412386>
- [29] Q. Zeng, J. Li, Q. Mou, Effect of FeO on spinel crystallization and chromium stability in stainless steel-making slag, *JOM*, 71 (7) (2019) 2331-2337.
<https://doi.org/10.1007/s11837-019-03465-0>
- [30] C. Han, Y. Jiao, Q. Wu, Kinetics and mechanism of hexavalent chromium removal by basic oxygen furnace slag, *Journal of Environmental Sciences*, 46 (8) (2016) 63-71. <https://doi.org/10.1016/j.jes.2015.09.024>
- [31] V. Breu, M. Clozel, K. Burri, Reduction of aqueous transition metal species on the surfaces of Fe(II)-containing oxides, *Geochimica Et Cosmochimica Acta*, 60 (20) (1996) 3799-3814.
[https://doi.org/10.1016/0016-7037\(96\)00213-X](https://doi.org/10.1016/0016-7037(96)00213-X)
- [32] J. Nell, J. Villiers, T-PO₂ topologic analysis of phase relations in the system CaO-CrO-Cr₂O₃-SiO₂, *Journal of the American Ceramic Society*, 76 (9) (2010) 2193-2200.
<https://doi.org/10.1111/j.1151-2916.1993.tb07754.x>
- [33] AM. Mirzayousef-Jadid, K. Schwerdtfeger, Redox equilibria of chromium in calcium silicate base melts, *Metallurgical and Materials Transactions B*, 40(4) (2009) 533-543. <https://doi.org/10.1007/s11663-009-9225-3>
- [34] M. I. Domínguez, F. Romero-Sarria, M. A. Centeno, Physicochemical characterization and use of wastes from stainless steel mill, *Environmental Progress & Sustainable Energy*, 29 (4) (2010) 471-480.
<https://doi.org/10.1002/ep.10435>



UTICAJ BINARNE BAZNOSTI NA POJAVU HROMA U ŠLJACI NERĐAJUĆEG ČELIKA

Q. Zeng ^a, J.-L. Li ^{a, b, c, *}, G.-J. Ma ^a, H.-Y. Zhu ^a

^a Glavna državna laboratorija za vatrostalne materijale i metalurgiju, Univerzitet nauke i tehnologije u Vuhanu, Vuhan, Kina

^b Glavna laboratorija za nove procese proizvodnje gvožđa i čelika u provinciji Hubei, Univerzitet nauke i tehnologije u Vuhanu, Vuhan, Kina

^c Glavna laboratorija Ministarstva obrazovanja za crnu metalurgiju i korišćenje resursa, Univerzitet nauke i tehnologije u Vuhanu, Vuhan, Kina

Apstrakt

Sveobuhvatno iskorišćenje šljake nerđajućeg čelika (SSS) ograničeno je zbog rizika luženja Cr^{6+} . Na osnovu proučavanja mikrostrukture sintetičke šljake (SS) sa sadržajem Cr_2O_3 uz pomoć XRD, SEM-EDS, i Image pro, istraživan je uticaj binarne baznosti na pojavu hroma u SSS. Rezultati su pokazali da binarna baznost ima značajan uticaj na osobine kristala spinela. Postojala je pozitivna korelacija između sadržaja kalcijuma u kristalima spinela i SS baznosti. Veličina kristala spinela varirala je od velikih do malih, i pojava taloženja se menjala kako je baznost rasla. Osim toga, sa baznošću se menjala i pojava hroma. Pri nižoj baznosti hrom se proizvodio u kristalima spinela, ali kako je baznost rasla do 3.0, hrom se taložio kao kalcijum hromat. S obzirom na odnos između ponašanja hroma pri luženju kao i na njegovo pojavljivanje, povećanjem baznosti je došlo do većeg luženja Cr^{6+} .

Ključne reči: Šljaka nerđajućeg čelika (SSS); Heksavalentni hrom; Kristali spinela; Binarna baznost

